PAPER

Phase Selection in Round-Robin Scheduling Sequence for Distributed Antenna System

Go OTSURU[†a)], ***Student Member and*** **Yukitoshi SANADA**[†b)], ***Fellow***

SUMMARY One of key technologies in the fifth generation mobile communications is a distributed antenna system (DAS). As DAS creates tightly packed antenna arrangements, inter-user interference degrades its spectrum efficiency. Round-robin (RR) scheduling is known as a scheme that achieves a good trade-off between computational complexity and spectrum efficiency. This paper proposes a user equipment (UE) allocation scheme for RR scheduling. The proposed scheme offers low complexity as the phase of UE allocation sequences are predetermined. Four different phase selection criteria are compared in this paper. Numerical results obtained through computer simulation show that maximum selection, which sequentially searches for the phase with the maximum tentative throughput realizes the best spectrum efficiency next to full search. There is an optimum number of UEs which obtains the largest throughput in single-user allocation while the system throughput improves as the number of UEs increases in 2-user RR scheduling.

key words: *distributed antenna system, round-robin scheduling*

1. Introduction

Recently, smartphones and tablet computers are widely used all over the world. Therefore, the amount of mobile traffic has increased explosively [1]. In addition, the Internet of Things (IoT) applications are gaining a lot of attention. The specifications in the fifth generation mobile communication system (5G) were determined in order to provide reliable wireless connections to those devices [1]. The spectrum efficiency of the 5G system must at least triple that of the previous generation [2]. Distributed antenna systems (DAS) have been investigated for achieving such high spectrum efficiency since they improve efficiency as the number of antennas increases [3], [4].

Moreover, channel conditions between user equipmets (UEs) and base stations vary independently. Therefore, spectrum efficiency also depends on the allocation of UEs and the selection of serving antennas [5]. In [6] and [7] scheduling schemes for a DAS based cellular system have been investigated. The research in [6] has demonstrated a UE allocation scheme with a dedicated hardware. In this research, each antenna selects a UE that achieves the highest throughput. The iteration of UE selection enables the system throughput to be close to the optimum. In [7], Max-C/I scheduling, proportional fair (PF) scheduling, and round-robin (RR) scheduling are compared. RR scheduling is less complex, but it can match the throughput and fairness of PF scheduling. However, in this research no UE allocation sequence in RR scheduling is taken into account.

This paper proposes a UE allocation scheme for the RR scheduling in the DAS. The proposal is intended for user in limited areas such as the those in factories [8], [9]. Thus, for low complexity, the proposed scheme sequentially determines UE allocation over multiple cells with distributed antennas (DAs) and it selects only the phase of the predetermined UE allocation sequence in each macro cell. Four different phase selection criteria are compared in this paper. The performance of the RR scheduling for allocating two users was presented in [10]. This paper evaluates the performance of the proposed scheme in detail and compares the tendencies of system throughputs in one user and two user allocation cases.

This paper is organized as follows. Section 2 describes the system model and the scheduling schemes. Section 3 explains simulation conditions. Numerical results obtained through computer simulation are then presented. Section 4 gives our conclusions.

2. System Description

2.1 Cell Model

A hexagonal seven-cell model shown in Fig. 1 is assumed.

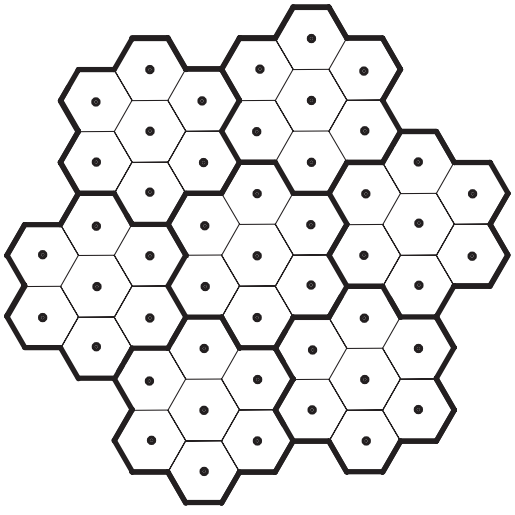

Fig. 1 Cell model with DAS.

Manuscript received October 23, 2019.
Manuscript revised January 16, 2020.
Manuscript publicized March 25, 2020.

[†]The authors are with the Dept. of Electronics and Electrical Engineering, Keio University, Yokohama-shi, 223-8522 Japan.
a) E-mail: gootsuru@snd.elec.keio.ac.jp
b) E-mail: sanada@elec.keio.ac.jp

DOI: 10.1587/transcom.2019EBP3222

One macro cell consists of seven micro cells and each DA is placed at the center of each micro cell. The number of DAs in each macro cell is $N_A = 7$. All DAs are connected to a central unit (CU). Interference only from adjacent macro cells is assumed to be known to the CU. Also, RR scheduling is adopted in an orthogonal frequency division multiplexing (OFDM) system for the allocation of UEs over resource blocks (RBs). Within the macro cell multiple UEs can be assigned to each RB and served by multiple DAs.

2.1.1 RR Scheduling

Suppose that the number of users in a macro cell is N_U and the number of users allocated to each RB is N_S, the total number of UE combinations is ${}_{N_U}\mathrm{C}_{N_S}$. The RR scheduling allocates UEs according to a UE allocation sequence with the length of ${}_{N_U}\mathrm{C}_{N_S}$.

2.1.2 Antenna Selection

Each UE is connected by one of the DAs that can realize the highest throughput at each RB as shown in Fig. 2. This is represented by a coefficient, P^r_{nm}. P^r_{nm} for the m-th DA to the n-th UE in the r-th RB is given as

$$P^r_{nm} = \begin{cases} 1 & (m = m^r_n) \\ 0 & (m \neq m^r_n) \end{cases} \tag{1}$$

where m^r_n is the selected DA corresponding to the n-th UE in the r-th RB. Thus, the signal for the n-th UE in the r-th RB is transmitted only from the m^r_n-th antenna. The transmit signal to the n-th UE in the l-th subcarrier of the r-th RB is represented by $x^{rl}_n(k^{rl}_n)$, where $k^{rl}_n (0 \leq k^{rl}_n \leq K^r_n - 1)$ is the constellation point index of the symbol and K^r_n is the modulation order for the n-th UE in the r-th RB.

Assuming that the RR scheduling with the phase of δ is applied, the received signal for the ν-th UE is given by

$$y^{rl}_\nu = h^{rl}_{\nu m_\nu}\sqrt{P^r_{\nu m_\nu}}x^{rl}_\nu(k^{rl}_n) + \sum_{m=1}^{N_A}\sum_{n\in\{\mu^r_\delta\},n\neq\nu} h^{rl}_{nm}\sqrt{P^r_{nm}}x^{rl}_n(k^{rl}_n) + z^{rl}_\nu \tag{2}$$

where $h^{rl}_{\nu m_\nu}$ is the channel response between the m-th DA and the n-th UE, z^{rl}_ν is the additive white Gaussian noise (AWGN) with a mean of zero and a variance of σ^2 on the l-th subcarrier of the r-th RB, and $\{\mu^r_\delta\}$ is the set of N_S UE indexes allocated to the r-th RB based on the RR scheduling sequence with the initial phase of δ. The details of the RR scheduling is explained in Sect. 2.2.

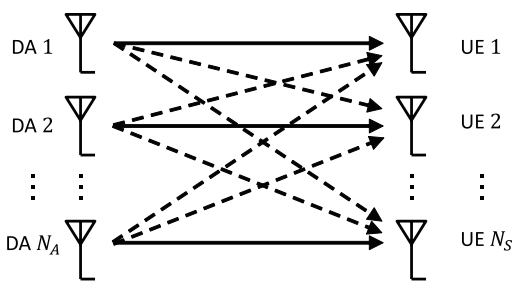

Fig. 2 Signal and interference.

The throughput for the ν-th UE in the l-th subcarrier of the r-th RB is calculated with as

$$\hat{T}^{rl}_\nu(\delta, m^r_\nu) = \log_2\left(1 + \frac{P^r_{nm}}{\sum_{m=1}^{N_A}\sum_{n\in\{\mu^r_\delta\},n\neq\nu} P^r_{nm} + \sigma^2}\right) \tag{3}$$

This is the tentative throughput for antenna allocation without taking inter-cell interference into account as it is determined after the allocation of DAs to UEs in the adjacent cells. The sum of the throughputs over the subcarriers and the allocated UEs in the r-th RB, $\hat{T}^r_{sum}(\delta, m^r_1, \cdots, m^r_{N_S})$, is then given by

$$\hat{T}^r_{sum}(\delta, m^r_1, \cdots, m^r_{N_S}) = \sum_{l\in\{l^r\}}\sum_{n\in\{\mu^r_\delta\}} \hat{T}^{rl}_n(\delta, m^r_n) \tag{4}$$

where $\{l^r\}$ is the set of subcarrier indexes in the r-th RB. The DAs are selected for N_S UEs to maximize the total throughput, $\hat{T}^r_{sum}(\delta, m^r_1, \cdots, m^r_{N_S})$. This is described as

$$\{m^r_1, \cdots, m^r_{N_S}\} = \underset{\hat{m}^r_1, \cdots, \hat{m}^r_{N_S}}{\arg\max}\ T^r_{sum}(\delta, \hat{m}^r_1, \cdots, \hat{m}^r_{N_S}) \tag{5}$$

where $\hat{m^r_n}$ is the antenna index allocated to the n-th UE in the r-th RB.

2.1.3 Throughput Calculation

Different from the tentative throughput, interference from other macro cells is included in the evaluation of the system throughput. The throughput for the ν-th UE in the l-th subcarrier of the r-th RB corresponding to the phase of δ, $T^{rl}_\nu(\delta, m^r_\nu)$, is given by

$$T^{rl}_\nu(\delta, m^r_\nu) = \log_2\left(1 + \frac{P^r_{nm}}{\sum_{m=1}^{N_A}\sum_{n\in\{\mu^r_\delta\},n\neq\nu} P^r_{nm} + {\eta^{rl}_\nu}^2}\right) \tag{6}$$

where η^{rl}_ν is the sum of the noise and the interference from the outer macro cells to the ν-th UE in the l-th subcarrier of the r-th RB. The total sum of the throughputs over the subcarriers and the allocated UEs in the r-th RB at the c-th macro cell, $T_c(\delta_c)$, is given by

$$T_c(\delta) = \sum_r \sum_{l\in\{l^r\}} \sum_{n\in\{\mu^r_{\delta_c}\}} T^{rl}_n(\delta_c, m^r_n). \tag{7}$$

Therefore, the system throughput over seven macro cells normalized by the number of the macro cells and the subcarriers

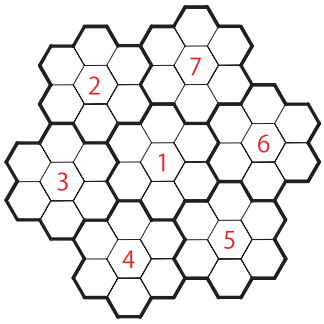

Fig. 3 Order of sequential RR scheduling.

Table 1 UE allocation sequence.

	UE allocated to RB			
Phase	UE 1	UE 2	$\cdots$	UE N_S
0	1	2	$\cdots$	N_S
1	1	2	$\cdots$	N_S+1
$\vdots$	$\vdots$	$\vdots$	$\ddots$	$\vdots$
${}_{N_U}\mathrm{C}_{N_S}-1$	N_U-N_S+1	N_U-N_S+2	$\cdots$	N_U

is given as

$$T = \frac{1}{7}\cdot\frac{1}{N_{SC}}\sum_{c=1}^{7} T_c(\delta_c) \tag{8}$$

where N_{SC} is the number of the subcarriers.

2.2 Proposed RR Scheduling

The proposed RR scheduling selects the phase of the UE allocation sequence. The phase selection is carried out in each macro cell sequentially over multiple macro cells. The order of the sequential phase selection is shown in Fig. 3.

In order to improve the system throughput with the proposed RR scheduling, the initial phase is determined in one of the seven macro cells at each timeslot. The initial phases of seven macro cells are then renewed over seven timeslots and the interval of seven timeslots is here called as a period. For all the RBs during each timeslot, UEs are allocated based on the sequence with the initial phase. An example of the UE allocation sequence is presented in Table 1. The numbers in the columns of UE n is the UE index allocated as the n-th user. The UEs allocated to the RBs are determined by consecutively extracting the UE indexes from the table in the ascending order of the phase and the initial phase is selected according to the system throughput. The phase index returns to the top if it reaches the bottom of the table.

2.2.1 Throughput Estimation

Suppose that the expected throughput for the ν-th UE in the l-th subcarrier of the r-th RB corresponding to the initial phase, δ, is represented as $\bar{T}_\nu^{rl}(\delta, m_\nu^r)$. The total sum of the expected throughput over all the UEs and the subcarriers of the RBs for the c-th macro cell is calculated from Eq. (6) and is given by

$$\bar{T}_c(\delta_c) = \sum_r \sum_{l\in\{l^r\}} \sum_{n\in\{\mu_{\delta_c}\}} \bar{T}_n^{rl}(\delta_c, m_n^r). \tag{9}$$

The expected system throughput corresponding to the set of the initial phases, $\{\delta_c\}$, over the macro cells is then given by

$$\bar{T}(\delta_1,\cdots,\delta_7) = \sum_{c=1}^{7}\bar{T}_c(\delta_c). \tag{10}$$

In this paper, four different criteria to the expected throughputs are applied in the initial phase selection.

2.2.2 Full Search

Full search calculates all the combinations of the initial phases over the seven macro cells. Since the length of the UE allocation sequence is ${}_{N_U}\mathrm{C}_{N_S}$, the number of combinations in seven macro cells is $({}_{N_U}\mathrm{C}_{N_S})^7$.

2.2.3 Random Selection

Random selection selects the initial phases in all the macro cells randomly and sequentially. Therefore, no throughput is estimated over all the periods.

2.2.4 Maximum Selection

For low complexity, the proposed scheme selects the phases of the UE allocation sequence over multiple macro cells sequentially and it is repeated iteratively. Suppose that t is the time index and $\hat{\delta}_c^{(t)}$ is the phase selected in the c-th macro cell at the t-th time index, the sum of the tentative throughputs given by the selection of the initial phase at the c-th macro cell, $\bar{T}(\hat{\delta}_1^{(t)},\cdots,\hat{\delta}_{c-1}^{(t)},\hat{\delta}_c,\hat{\delta}_{c+1}^{(t-1)},\cdots,\hat{\delta}_7^{(t-1)})$, is calculated from Eq. (10) for all of $\delta_c\,(0\le\delta_c\le{}_{N_U}\mathrm{C}_{N_S}-1)$. The maximum selection selects the phase with the largest expected throughput. The maximum selection is defined as

$$\hat{\delta}_c^{(t)} = \arg\max_{\hat{\delta}_c} \bar{T}(\hat{\delta}_1^{(t)},\cdots,\hat{\delta}_{c-1}^{(t)},\hat{\delta}_c,\hat{\delta}_{c+1}^{(t-1)},\cdots,\hat{\delta}_7^{(t-1)}). \tag{11}$$

Since this criterion selects the phase sequentially, the system throughput may fall into a local optimum. The throughput estimation is conducted $7({}_{N_U}\mathrm{C}_{N_S})$ times at each period.

2.2.5 Selection with Gibbs Sampling

The selection with Gibbs sampling uses the expected throughput, $\bar{T}(\hat{\delta}_1^{(t)},\cdots,\hat{\delta}_{c-1}^{(t)},\hat{\delta}_c,\hat{\delta}_{c+1}^{(t-1)},\cdots,\hat{\delta}_7^{(t-1)})$, corresponding to the set of the phases, $\{\delta_c\}$. The probability of selecting the phase, $\hat{\delta}_c$, in the c-th macro cell is given by

$P(\hat{\delta}_c)$

Table 2 Simulation conditions.

Cell layout	Hexagonal 7-cell model
Inter-antenna distance	50, 100, 150, 200 m
Minimum distance between UE and DA	5 m
Height of antennas	10 m
Height of UEs	1.5 m
System bandwidth	4.32 MHz
RB bandwidth	180 kHz
Number of RBs	24
Number of subcarriers per RB	12
Transmit power	30 dBm
Distance dependent path loss	$140.7 + 36.7 \log_{10}(R)$ dB R:Distance (km)
Shadowing standard deviation	8 dB
Channel model	Intersite cell: One-path Rician From outer cell: Six-path Rayleigh
Receiver noise density	−174 dB/Hz
Allocation	Single-user allocation 2-user allocation
Number of UEs per macro cell	3, 5, 10, 15, 20
Temperature coefficient K	100, 1000, 10000

$$= \frac{\exp\left(\bar{T}(\hat{\delta}_1^{(t)}, \cdots, \hat{\delta}_{c-1}^{(t)}, \hat{\delta}_c, \hat{\delta}_{c+1}^{(t-1)}, \cdots, \hat{\delta}_7^{(t-1)})/K\right)}{\sum_{\hat{\delta}_c=0}^{N_U C_{N_S}-1} \exp\left(\bar{T}(\hat{\delta}_1^{(t)}, \cdots, \hat{\delta}_{c-1}^{(t)}, \hat{\delta}_c, \hat{\delta}_{c+1}^{(t-1)}, \cdots, \hat{\delta}_7^{(t-1)})/K\right)} \tag{12}$$

where K is the temperature coefficient. If K is large, this criterion tends to perform as random selection. If K is small, this criterion works similarly as maximum selection. The throughput estimation is carried out $7({}_{N_U}C_{N_S})$ times at each period.

The advantage of applying Gibbs sampling is that there is a certain probability that the search result may escape from a local optimum even if the search falls into it and the set of the phases approaches the global optimum.

3. Numerical Results

3.1 Simulation Conditions

The hexagonal 7-cell model is assumed as a cell layout. The inter-antenna distance is selected from 50, 100, 150, or 200 meters as 256QAM signals with less than 50 MHz bandwidth can be transported over a LAN cable by up to 200 meters [11]. The height of the DAs is 10 meters and the height of the UEs is 1.5 meters. The system bandwidth is 4.32 MHz and the RB bandwidth is 180 kHz. The number of RBs is 24 and the number of subacarriers per RB is 12. The transmit power per a antenna is set to 30 dBm. The decay coefficient of the propagation loss is 36.7. The shadowing deviation is 8 dB. An one-path Rician fading channel model is assumed for intra cell and a six-path Rayleigh fading channel with an exponential decay profile is assumed for interference from outer cells. The root-mean-square (RMS) delay spread is seto to 1 μs. The receiver noise density is set to −174 dB/Hz. A single-user allocation ($N_S = 1$) and a 2-user allocation ($N_S = 2$) are evaluated. The number of UEs per macro cell is 3, 5, 10, 15, or 20. The temperature coefficient, K, is set as 100, 1000, or 10000. The average system throughput per subcarrier per cell is evaluated for different phase selection criteria unless it is specified.

To measure the effect of temperature coefficient, the selection probability of the phase versus the estimated relative throughput is evaluated. The estimated relative throughput with the initial phase, $\hat{\delta}_c$, in the c-th macro cell is given by

$$R(\hat{\delta}_c) = \frac{\bar{T}(\hat{\delta}_1^{(t)}, \cdots, \hat{\delta}_{c-1}^{(t)}, \hat{\delta}_c, \hat{\delta}_{c+1}^{(t-1)}, \cdots, \hat{\delta}_7^{(t-1)})/K}{\sum_{\hat{\delta}_c=0}^{N_U C_{N_S}-1} \bar{T}(\hat{\delta}_1^{(t)}, \cdots, \hat{\delta}_{c-1}^{(t)}, \hat{\delta}_c, \hat{\delta}_{c+1}^{(t-1)}, \cdots, \hat{\delta}_7^{(t-1)})/K}. \tag{13}$$

3.2 Single-User RR Scheduling

3.2.1 Number of Search Iterations

The system throughput characteristics with single-user RR scheduling versus the number of search iterations are presented in Figs. 4 and 5. The number of UEs are 3 or 10 and the inter-antenna distance is 100 meters. The system throughput for the full search is included in Fig. 4. The maximum selection achieves the largest throughput except the full search. The system throughput for the maximum selection reaches 99% of that for the optimum system throughput even the number of search iterations is small. This implies that not many local optimums exist in the search space. Therefore, the system throughput for the Gibbs sampling with the smaller temperature parameters is larger. The system throughput of the random selection is equivalent with those of the Gibbs sampling with $K = 100$ and $K = 1000$. The average phase selection probability in the Gibbs sampling versus the estimated relative throughput is presented in Fig. 6. The number of UEs is 10, the inter-antenna distance is 100 meters, and the number of search iterations is 22. In single-user RR scheduling, the number of combinations for the initial phases is equivalent to the number of UEs and each criterion for the phase selection picks up the initial phases from the candidates of the initial phases. The Gibbs sampling with $K = 1000$ or $K = 10000$ selects the initial phase almost randomly while the Gibbs sampling with $K = 100$ tends to select the initial phases with higher throughputs.

The cumulative distribution function (CDF) of the system throughput is shown in Fig. 7. The figure indicates that the maximum selection is also superior to the other criteria in terms of 5%-CDF throughput. Maximum selection achieves higher throughput than the others criteria including the selection with Gibbs sampling. The CDF of the user throughput is shown in Fig. 8. The users with the best throughput and with the worst throughput among five users are presented in the figure. Maximum selection achieves superior performance as compared to the other selection criteria for both user cases. Gibbs sampling is able to escape from a local optimum and

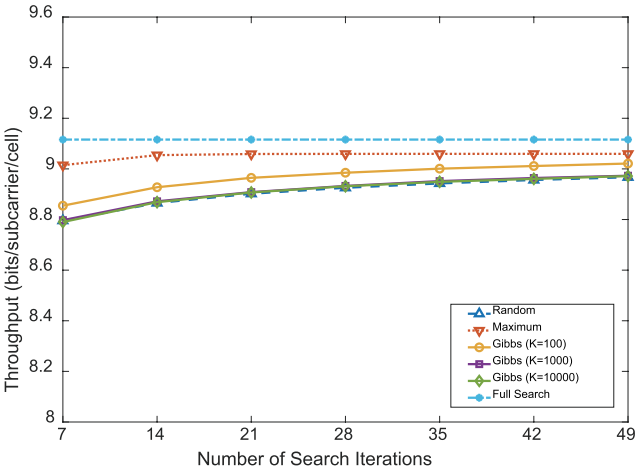

Fig. 4 System throughput vs. no. of search iterations (single-user RR scheduling, $N_U = 3$, inter-antenna distance 100 m).

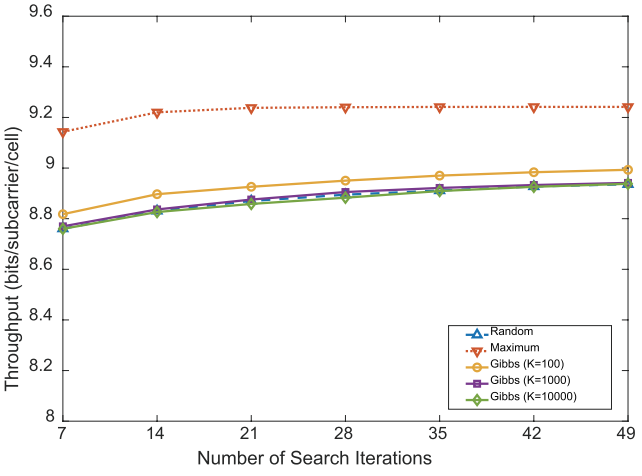

Fig. 5 System throughput vs. no. of search iterations (single-user RR scheduling, $N_U = 10$, inter-antenna distance 100 m).

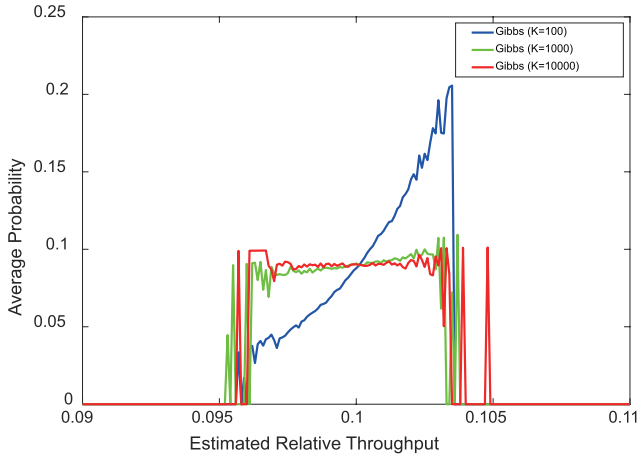

Fig. 6 Average phase selection probability vs. relative throughput (single-user RR scheduling, $N_U = 10$, 22 search iterations, inter-antenna distance 100 m).

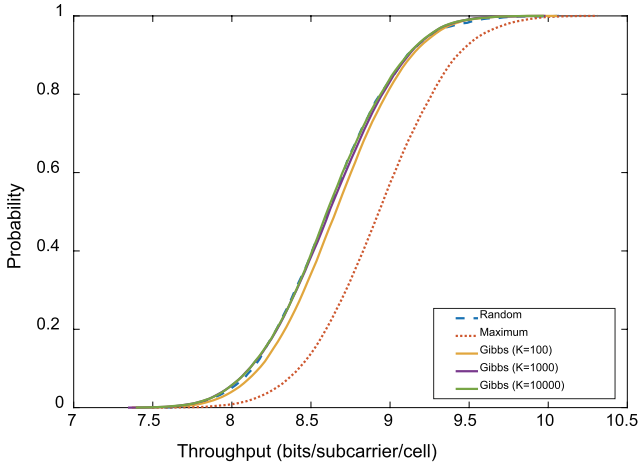

Fig. 7 CDF of throughput(single-user RR scheduling, $N_U = 10$, 14 search iterations, inter-antenna distance 100 m).

the selection with Gibbs sampling tends to indicate superior performance. However, in the assumed system, the local optimum rarely exists and the throughput difference between the optimum and the local optimum is small. The ratio of the local optimums is 0.62% among all the combinations. The CDF of the throughput difference between the optimum when $N_S = 3$ and the local optimum is shown in Fig. 9. The search result hardly falls into the local optimum and the throughput difference is small even if the search falls into it. Consequently, maximum selection outperforms the other criteria.

3.2.2 Effect of Number of UEs

In single-user RR scheduling, the system throughput characteristics versus the number of users are shown in Fig. 10. The number of search iterations is 14 and the inter-antenna distance is 100 meters. If the number of UEs increases from 3 to 15, the system throughput increases. If the number of UEs increases from 15 to 20, the system throughput deteriorates. The reason is that the allocated UEs over all the RBs includes more versatile combinations if the number of UEs increases. Therefore, it is harder to assign better combinations of the UEs over the macro cells just by selecting the initial phase of the sequences.

3.2.3 Effect of Inter-Antenna Distance

The system throughput versus the inter-antenna distance is shown in Fig. 11. The number of UEs is 10 and the number of search iterations is 14. If the inter-antenna distance is longer, the system throughput improves. This is because the interference from the outer macro cells decreases owing to the propagation loss. When the inter-antenna distance changes from 150 meters to 200 meters, almost the same system throughput is maintained. Thus, the inter-cell interference is not significant if the inter-antenna distance is larger. However, the distance between the DA and the UE also increases and the received signal power reduces. Thus,

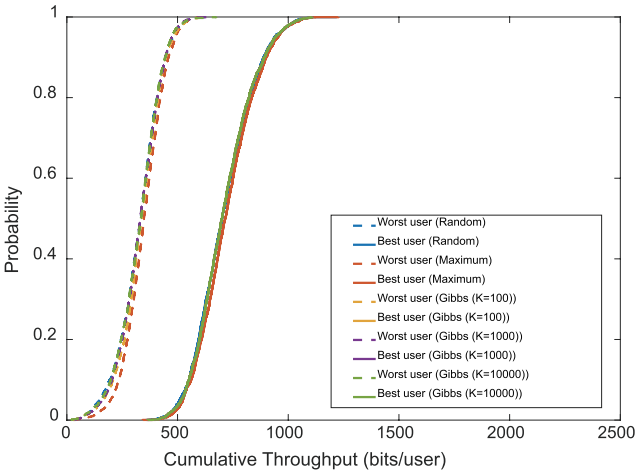

Fig. 8 CDF of user throughput(single-user RR scheduling, $N_U = 5$, 14 search iterations, inter-antenna distance 100 m).

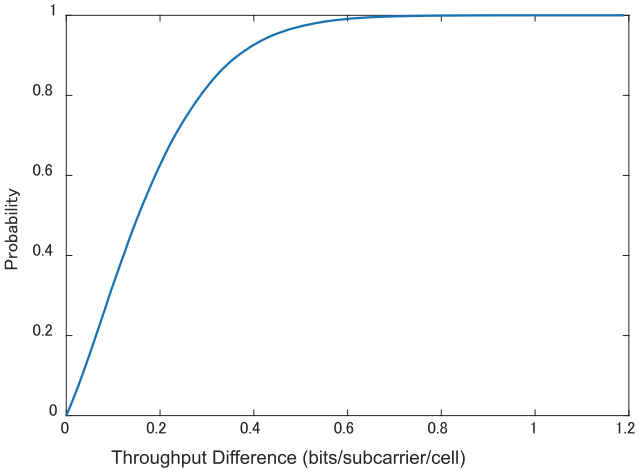

Fig. 9 CDF of difference between optimum and local optimum (single-user RR scheduling, $N_U = 3$, inter-antenna distance 100 m).

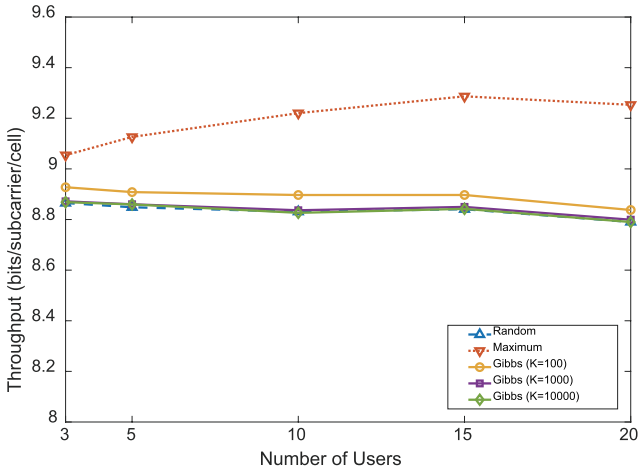

Fig. 10 System throughput vs. no. of users (single-user RR scheduling, 14 search iterations, inter-antenna distance 100 m).

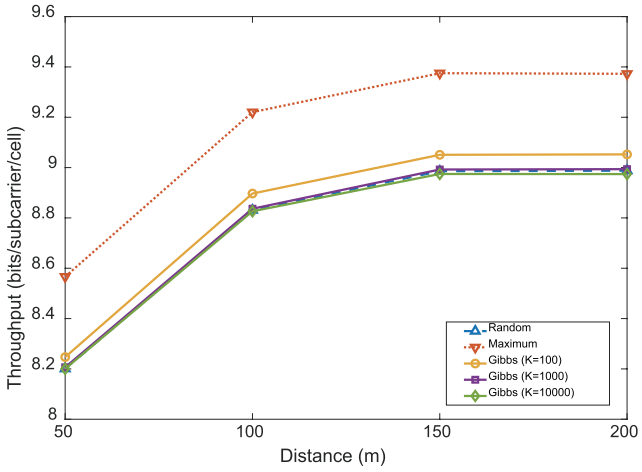

Fig. 11 System throughput vs. inter-antenna distance (single-user RR scheduling, $N_U = 10$, 14 search iterations).

less improvement in the system throughput is observed.

3.3 2-User RR Scheduling

3.3.1 Number of Search Iterations

The system throughput versus the number of search iterations for 2-user RR scheduling is shown in Figs. 12 and 13. The number of UEs is 3 or 10 and the inter-antenna distance is 100 meters. The same as the system throughput in single-user RR scheduling the maximum selection indicates the largest throughput and it reaches 99.5% of that for the full search as shown in Fig. 12. As for the system throughput with the Gibbs sampling the same tendencies can be observed with those in single-user RR scheduling. The system throughput for the Gibbs sampling with the smaller temperature parameter is larger. The average phase selection probability in the Gibbs sampling versus the estimated relative throughput is presented in Fig. 14. The number of UEs is 10, the inter-antenna distance is 100 meters, and the number of search iterations is 22. In 2-user RR scheduling, the number of combinations for the initial phases is ${}_{10}C_2$ and each criterion for the phase selection picks up the initial phases from the candidates of the initial phases. The Gibbs sampling with $K = 1000$ or $K = 10000$ selects the initial phase almost randomly while the Gibbs sampling with $K = 100$ tends to select the initial phases with higher throughputs.

The CDF of the system throughput is shown in Fig. 15. The figure indicates that the maximum selection is also superior to the other criteria in terms of 5%-CDF throughput. Maximum selection achieves higher throughput than the others criteria including the selection with Gibbs sampling. The CDF of the user throughput is shown in Fig. 16. The users with the best throughput and with the worst throughput among five users are presented in the figure. Different from single-user allocation, maximum selection shows the equivalent performance as compared to the other selection criteria for the worst throughput user while it realizes superior performance for the best throughput user. Therefore, the

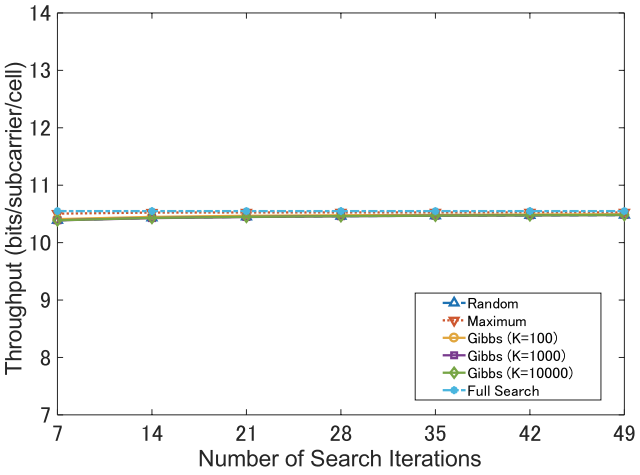

Fig. 12 System throughput vs. no. of search iterations (2-user RR scheduling, $N_U = 3$, inter-antenna distance 100 m).

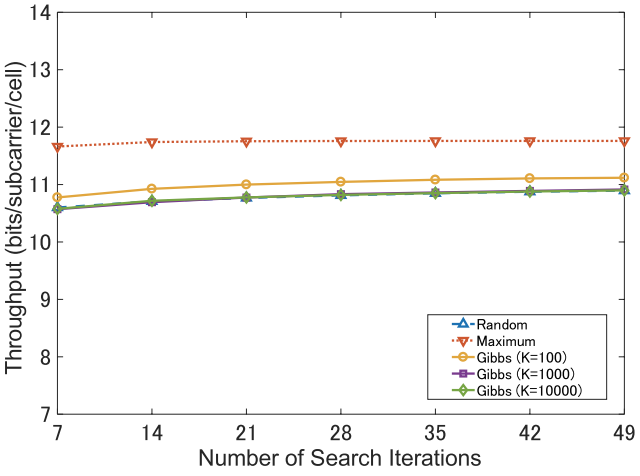

Fig. 13 System throughput vs. no. of search iterations (2-user RR scheduling, $N_U = 10$, inter-antenna distance 100 m).

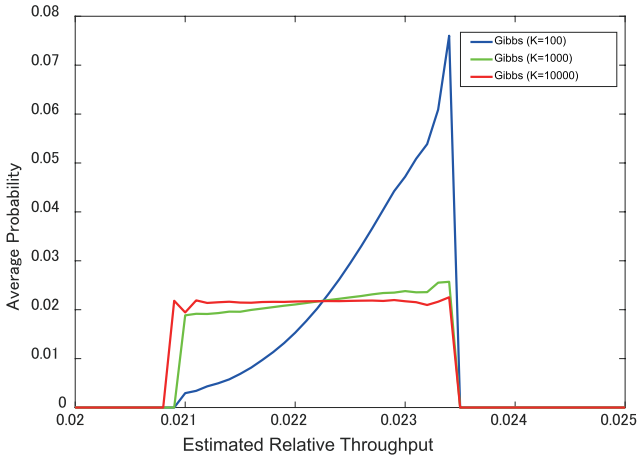

Fig. 14 Average phase selection probability vs. relative throughput (single-user RR scheduling, $N_U = 10$, 22 search iterations, inter-antenna distance 100 m).

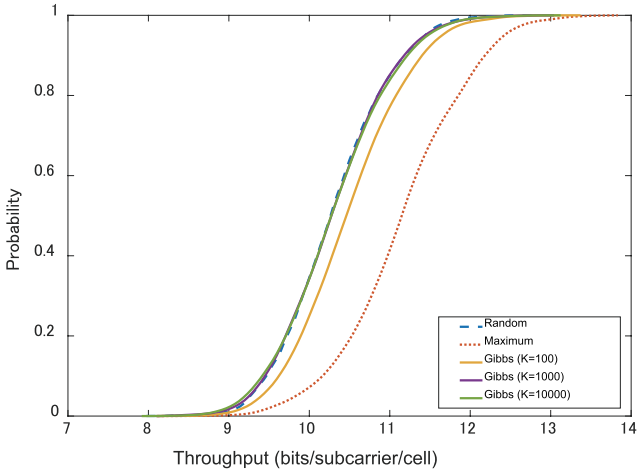

Fig. 15 CDF of throughput(2-user RR scheduling, $N_U = 10$, 14 search iterations, inter-antenna distance 100 m).

fairness among users deteriorates. Gibbs sampling is able to escape from a local optimum and the selection with Gibbs sampling tends to indicate superior performance. However, in the assumed system, the local optimum rarely exists and the throughput difference between the optimum and the local optimum is small. The ratio of the local optimums is 0.50% among all the combinations. The CDF of the throughput difference between the optimum and the local optimum when $N_S = 3$ is shown in Fig. 17. The search result hardly falls into the local optimum and the throughput difference is small even if the search falls into it. Consequently, maximum selection outperforms the other criteria.

3.3.2 Effect of Number of UEs

In 2-user RR scheduling, the system throughput versus the number of UEs are presented in Fig. 18. The number of the search iterations is 14 and the inter-antenna distance is 100 meters. Different from those in single-user RR scheduling, the system throughput increases as the number of UEs grows. This is because of the UE allocation sequence given in Table 1. In 2-user RR scheduling, the same UE index is allocated as UE 1 consecutively. Therefore, by selecting the initial phase of the sequence, the same UE can be allocated to the consecutive RBs and it is more possible to find better combinations of UEs over the macro cells and all the RBs.

3.3.3 Effect of Inter-Antenna Distance

The system throughput versus the inter-antenna distance is shown in Fig. 19. The number of UEs is 10 and the number or the search iterations is 14. If the inter-antenna distance is longer, the system throughput improves. The reason is that the interference from other macro cells decreases owing to the propagation loss as the inter-antenna distance is long. Different from those in single-user RR scheduling, when the inter-antenna distance changes from 150 meters to 200 meters, the system throughput still increases. In 2-user RR scheduling, the intra-cell interference among the DAs as well

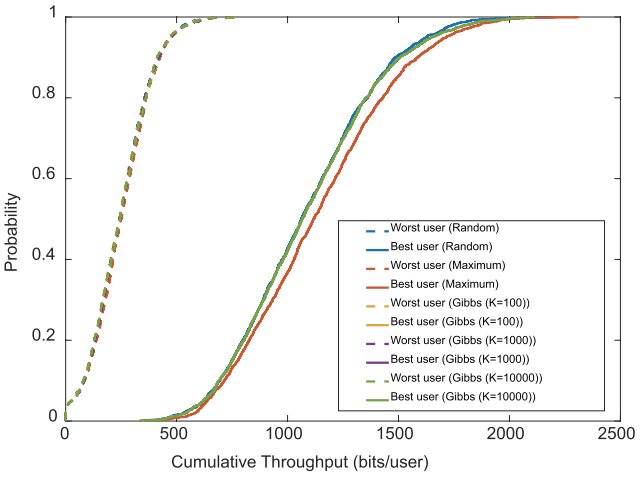

Fig. 16 CDF of user throughput(2-user RR scheduling, $N_U = 5$, 14 search iterations, inter-antenna distance 100 m).

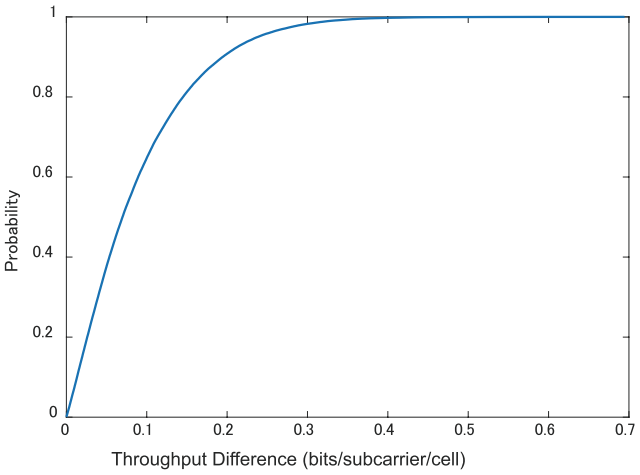

Fig. 17 CDF of difference between optimum and local optimum (2-user RR scheduling, $N_U = 3$, inter-antenna distance 100 m).

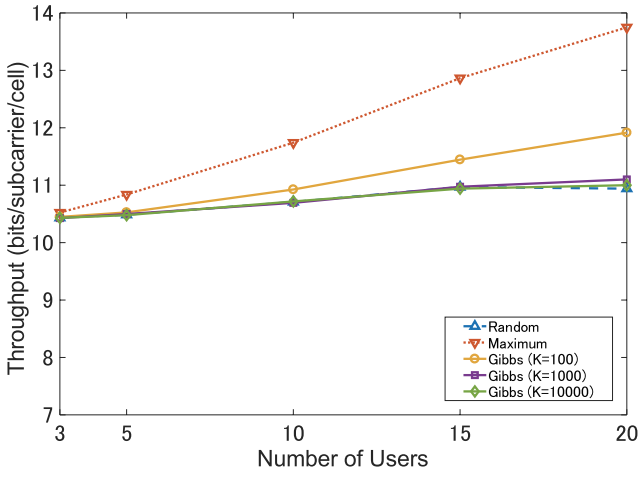

Fig. 18 System throughput vs. no. of users (2-user RR scheduling, 14 search iterations, inter-antenna distance 100 m).

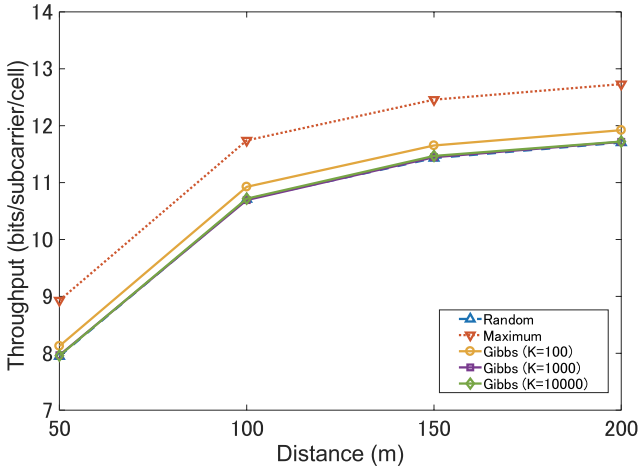

Fig. 19 System throughput vs. inter-antenna distance (2-user RR scheduling, $N_U = 10$, 14 search iterations).

as inter-cell interference reduces if the inter-antenna distance increases and the system throughput improves.

4. Conclusions

In this paper, the UE allocation scheme for the RR scheduling is proposed. The proposed scheme selects the initial phases of the UE allocation sequence over the macro cells sequentially. Four different phase selection criteria are compared in this paper. It has been shown through numerical results that the maximum selection achieves the largest throughputs and it reaches over 99% of that for the optimum selection when the number of UEs is three. There is an optimum number of UEs which obtains the largest throughput in single-user allocation while the system throughput improves as the number of UEs increases in 2-user RR scheduling. The system throughput improves as the inter-antenna distance increases especially in 2-user RR scheduling.

Acknowledgments

This work is supported in part by a Grant-in-Aid for Scientific Research (C) under Grant No. 19K04396 from the Ministry of Education, Culture, Sports, Science, and Technology of Japan.

References

[1] "Assessment of the global mobile broadband deployments and forecasts for international mobile telecommunications," ITU-R M.2243, March 2011.
[2] "IMT vision - Framework and overall objectives of the future development of IMT for 2020 and beyond," ITU-R M.2083-0, Sept. 2015.
[3] M.V. Clark, T.M. Willes, III, L.J. Greenstein, A.J. Rustako, Jr., V. Erceg, and R.S. Roman, "Distributed versus centralized antenna arrays in broadband wireless networks," IEEE 53rd Vehicular Technology Conference, May 2001.
[4] H. Matsuda, H. Tomeda, and F. Adachi, "Channel capacity of distributed antenna system using maximal ratio transmission," 5th IEEE

VTS Asia Pacific Wireless Communications Symposium, Aug. 2008.
[5] E. Dahlman, S. Parkvall, and J. Sköld, 4G:LTE/LTE-Advanced for Mobile Broadband Second Edition, Academic Press, New York, 2011.
[6] Y. Arikawa, H. Uzawa, T. Sakamoto, and S. Shigematsu, "High-speed radio-resource scheduling for 5G ultra-high-density distributed antenna systems," 2016 8th International Conference on Wireless Communications and Signal Processing, Oct. 2016.
[7] Y. Seki and F. Adachi, "Downlink capacity comparision of MMSE-SVD and BD-SVD for cooperative distributed antenna transmission using multi-user scheduling," IEEE 86th Vehicular Technology Conference, Sept. 2017.
[8] M. Matinmikko-Blue and M. Latva-aho, "Micro operators accelerating 5G deployment," 2017 IEEE International Conference on Industrial and Information Systems, Dec. 2017.
[9] K.B. Shashika Manosha, M. Matinmikko-Blue, and M. Latva-aho, "Framework for spectrum authorization elements and its application to 5G micro-operators," 2017 Internet of Things Business Models, Users, and Networks, Nov. 2017.
[10] G. Otsuru and Y. Sanada, "User allocation with round-robin scheduling sequence for distributed antenna system," IEEE 90th Vehicular Technology Conference 2019 Fall, Sept. 2019.
[11] S.H.R. Naqvi, A. Matera, L. Combi, and U. Spagnolini, "On the transport capability of LAN cables in all-analog MIMO-RoC fronthaul," IEEE Wireless Commun. Netw. Con., March 2017.

Go Otsuru was born in Nagasaki, Japan in 1995. He received his B.E. degree in electronics engineering from Keio University, Japan in 2019. Since April 2019, he has been a graduate student in School of Integrated Design Engineering, Graduate School of Science and Technology, Keio University. His research interests are mainly resource allocation.

Yukitoshi Sanada was born in Tokyo in 1969. He received his B.E. degree in electrical engineering from Keio University, Yokohama, Japan, his M.A.Sc. degree in electrical engineering from the University of Victoria, B.C., Canada, and his Ph.D. degree in electrical engineering from Keio University, Yokohama, Japan, in 1992, 1995, and 1997, respectively. In 1997 he joined the Faculty of Engineering, Tokyo Institute of Technology as a Research Associate. In 2000, he joined Advanced Telecommunication Laboratory, Sony Computer Science Laboratories, Inc, as an associate researcher. In 2001, he joined the Faculty of Science and Engineering, Keio University, where he is now a professor. He received the Young Engineer Award from IEICE Japan in 1997. His current research interests are in software defined radio, cognitive radio, and OFDM systems.